

# Supplementary information: On the role of hydrodynamic interactions in the engineered-assembly of droplet ensembles

Danny Raj M,<sup>\*a</sup> Abeynaya Gnanasekaran,<sup>b</sup> and Raghunathan Rengaswamy<sup>a</sup>

## 1 Lubrication forces and interface mobility

**Note: this section supplements the latter part of section 2 in the manuscript (Stability of droplet ensembles).** We show that mobility of droplet interfaces do not result in coalescence of droplets in the system under consideration.

Davis and Schoenberg<sup>1</sup>, in their study of approaching droplets in a viscous environment, showed that when interfaces are mobile, droplets can come in contact in finite time unlike the case of immobile interfaces where contact happens at the limit of  $t \rightarrow \infty$ . However, these results are derived for the case where a constant force acts on the two droplets facilitating approach. For the system under consideration in the manuscript, droplet-approach happens only when the background flow facilitates it; like in the case of a diverging channel geometry where droplets slow down as they move through the channel resulting in approach. In light of this difference in the way droplets are pushed together in our system of interest, the dynamics of approach have to be re-derived to understand the effect of mobility of droplet interface. In what follows, we first derive the approach dynamics for the case of constant forcing and then for that of modified forcing, more suitable for our system, and compare the results.

Consider the case where two droplets approach each other. The lubrication force between two droplets when the interfaces are completely mobile<sup>1</sup> is given by Eq 1. The terminology is very similar to that in ref<sup>1</sup>;  $\lambda\mu$  is the viscosity of the continuous phase,  $R$  the radius of the droplets,  $x_i$  and  $u_i$ , the position and velocity of droplet  $i$  (where  $i$  can be 1 or 2). Balancing the drag force due to the background flow and the lubrication force due to approach, we can get the governing equation for droplet motion as in Eq 3 and 4. By solving Eq 3 and 4 for the velocities of the droplets  $u_1$  and  $u_2$ , we get Eq 5 and 6, which can be solved simultaneously to get the dynamics of approach of the droplets  $\Delta x = (x_2(t) - x_1(t))$ . All the algebraic manipulations were done using the Mathematica<sup>©</sup> package<sup>2</sup>.

---

<sup>0a</sup> Department of chemical engineering, IISc Bangalore, Bengaluru 560012, Karnataka, India; E-mail: dannyrajm@iisc.ac.in

<sup>0b</sup> Department of chemical engineering, IIT Madras, Chennai 600036, Tamil Nadu, India

$$F_{1-2} = 16.5\lambda\mu R(u_1 - u_2)\sqrt{\frac{R}{x_2 - x_1 - 2R}} \quad (1)$$

$$(u_i - u_{i,0}) - \frac{F_{i-j}}{6\pi\mu R} = 0 \quad (2)$$

$$(u_1 - u_{1,0}) - 0.875\lambda(u_1 - u_2)\sqrt{\frac{R}{x_2 - x_1 - 2R}} = 0 \quad (3)$$

$$(u_2 - u_{2,0}) - 0.875\lambda(u_2 - u_1)\sqrt{\frac{R}{x_2 - x_1 - 2R}} = 0 \quad (4)$$

$$\frac{dx_1}{dt} = u_1 = \frac{u_{1,0} \left( 0.5\lambda\sqrt{\frac{R}{-2R-x_1+x_2}} - 0.57 \right) + 0.5\lambda u_{2,0}\sqrt{\frac{R}{-2R-x_1+x_2}}}{\lambda\sqrt{\frac{R}{-2R-x_1+x_2}} - 0.57} \quad (5)$$

$$\frac{dx_2}{dt} = u_2 = \frac{0.5\lambda u_{1,0}\sqrt{\frac{R}{-2R-x_1+x_2}} + u_{2,0} \left( 0.5\lambda\sqrt{\frac{R}{-2R-x_1+x_2}} - 0.57 \right)}{\lambda\sqrt{\frac{R}{-2R-x_1+x_2}} - 0.57} \quad (6)$$

The case discussed above involves a constant driving force given by  $\Delta u = (u_{1,0} - u_{2,0})$ , which continuously brings the droplets together (as shown in figure 1A and 2A). In our system (section 3.2 in manuscript), where the approach is primarily due to the diverging section of the channel, the driving force for the approach of the droplets is no longer a constant, but a function of space. Typically for a linearly diverging channel, the velocity profile (due to mass conservation) is  $(u_0 k/x)$  (as shown in figure 1B and 2B). Hence, for a modified driving force, as shown in Eq 7, we can derive the equations governing the motion of droplets (Eq 10 and 11).

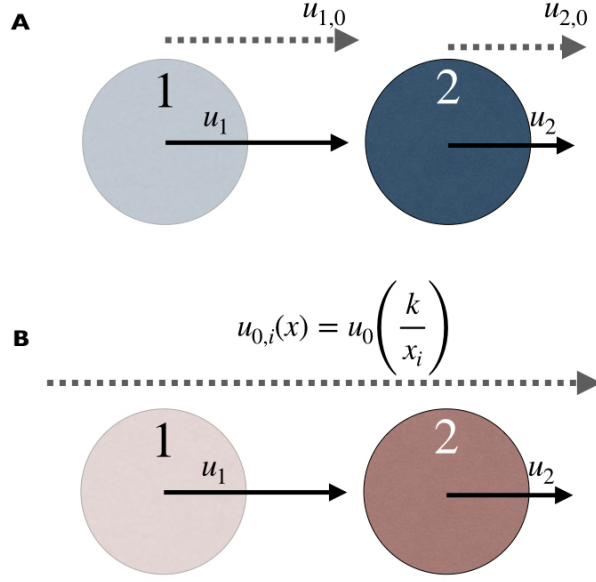


Figure 1: A- The case of constant driving force; B- Driving force in a linearly diverging channel

$$u_{i,0} = u_0 \left( \frac{k}{x_i} \right) \quad (7)$$

$$u_1 - u_0 \left( \frac{k}{x_1} \right) - 0.875\lambda(u_1 - u_2) \sqrt{\frac{R}{x_2 - x_1 - 2R}} = 0 \quad (8)$$

$$u_2 - u_0 \left( \frac{k}{x_2} \right) - 0.875\lambda(u_2 - u_1) \sqrt{\frac{R}{x_2 - x_1 - 2R}} = 0 \quad (9)$$

$$\frac{dx_1}{dt} = u_1 = \frac{ku_0 \left( x_2 \left( 0.5\lambda \sqrt{\frac{R}{-2R-x_1+x_2}} - 0.57 \right) + 0.5\lambda x_1 \sqrt{\frac{R}{-2R-x_1+x_2}} \right)}{x_1 x_2 \left( \lambda \sqrt{\frac{R}{-2R-x_1+x_2}} - 0.57 \right)} \quad (10)$$

$$\frac{dx_2}{dt} = u_2 = \frac{ku_0 \left( x_1 \left( 0.5\lambda \sqrt{\frac{R}{-2R-x_1+x_2}} - 0.57 \right) + 0.5\lambda x_2 \sqrt{\frac{R}{-2R-x_1+x_2}} \right)}{x_1 x_2 \left( \lambda \sqrt{\frac{R}{-2R-x_1+x_2}} - 0.57 \right)} \quad (11)$$

Figure 2C outlines the results of the simulation of Eq 3 and 4 and figure 2D that of Eq 10 and 11. Simulation was done for a wide range of parameter values and that which is shown in figure 2 is an exemplary case. Along with the case of mobile interface, that of an immobile interface (corresponding to the model system in section 22 in manuscript) and no-lubrication force cases are also plotted for comparison in figure 2. One can notice that, under constant forcing, contact is possible when droplets have fully mobile interfaces. The contact time is slightly higher than the case with no lubrication force (un-physical, but

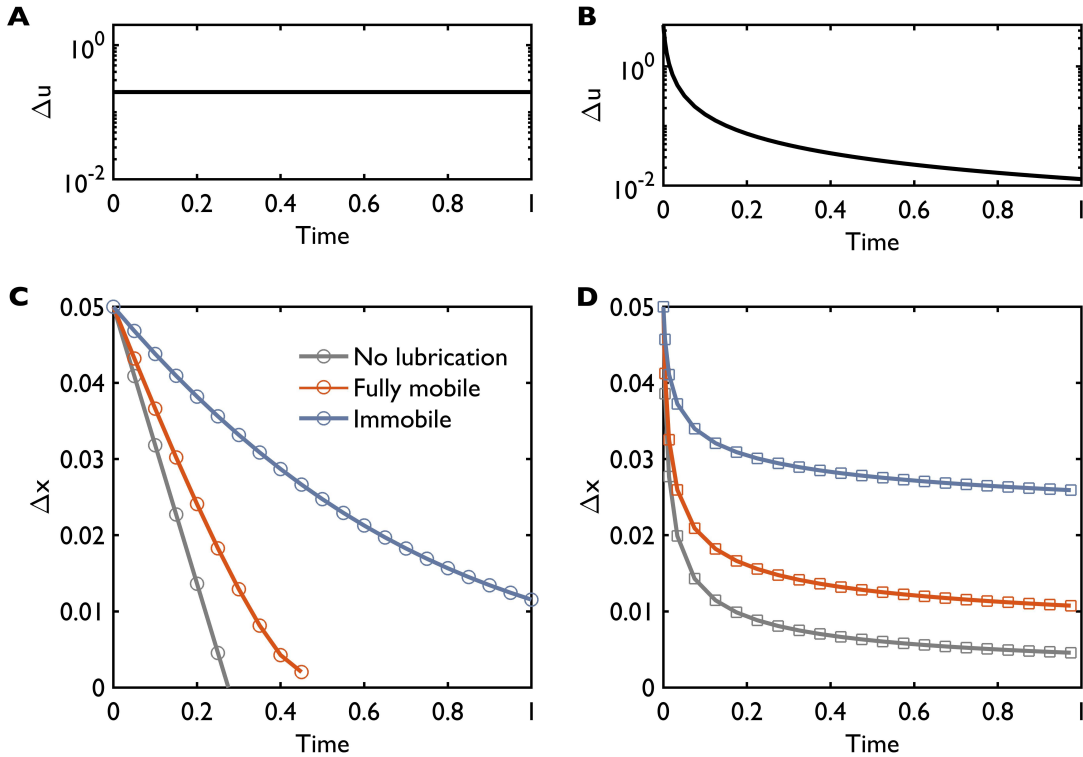


Figure 2: A- Constant forcing with time ( $u_{1,0} - u_{2,0}$ ); B- Forcing in a linearly diverging channel; C- Distance between the droplets as a function of time for the case of no lubrication force, lubrication force with fully mobile interface and immobile interface; D- Dynamics of approach in a diverging channel.

sets a lower bound on the contact time). In contrast the immobile case does not result in contact even for large times (not shown in the plot). However, when the forcing is modified to account for a linearly diverging channel, we see that contact is prevented because, the driving force becomes smaller as the droplets come closer. One can understand why this happens by observing factor  $x_1 x_2$  that has appeared in the denominator of Eq 10 and 11. This factor reduces the net driving force as the droplets move forward and together, in the channel. Hence, even the case without lubrication force does not result in contact. With any kind of lubrication force, approach is only further delayed. And hence, in our system there is no qualitative difference in the approach dynamics due to mobility of the droplet interface.

## 2 Metastability of droplet assemblies

### 2.1 Steady state characteristics of symmetric shapes

**Note: this section supplements section 3.1 of the manuscript.** In figure 4 of the manuscript, we see two types of shapes. First are the stable configurations which when perturbed return to the same state as its initial and second, other configurations that rearrange and go to the stable ones when disturbed slightly. Shen et al<sup>3</sup> were able to synthesize all the configurations listed in figure 4 of manuscript, the stable ones and the ‘unstable ones’.

While it is straight-forward to understand how one can make particles out of the stable configuration, it is un-clear for the latter case. We posit that this would be possible only if the dynamics around these ‘unstable states’ are slow- *metastable* (as discussed in section 3.1 of manuscript).

In this section, we show numerically that the symmetric equivalents of these shapes (without any perturbation), are indeed steady state solutions to the governing equations and unstable to perturbation. Hence, the dynamics about these states are slow and they get a meta-stable character that allows fusion into particles of that shape.

We consider all the ‘unstable’ configurations from figure 4 of the manuscript and without introducing any perturbation, taking the symmetric shape, solve the governing equations of the dynamics of droplets. We observe that except for the third structure in 3b, all the other shapes remain unchanged. This is a numerical route to confirming that the structures are indeed steady states to the governing equations. One should also note that a few of the structures considered in figure 3 are mirror images (about the direction perpendicular to the background flow, which in our case is the y-axis) of what is shown in figure 4 of the manuscript. This is because, the mirror image of a structure may not be a steady state to the governing equations as the long-range interaction is fore-aft asymmetric. The sharp change in the structure parameter at the beginning is due to the repulsive interactions that push the droplets away to the point where the repulsion interactions and attractive depletion interactions balance, without changing the shape of the configuration. However, with slight perturbation, all these structures shown here would relax to a stable steady configuration as shown in figure 4 of manuscript.

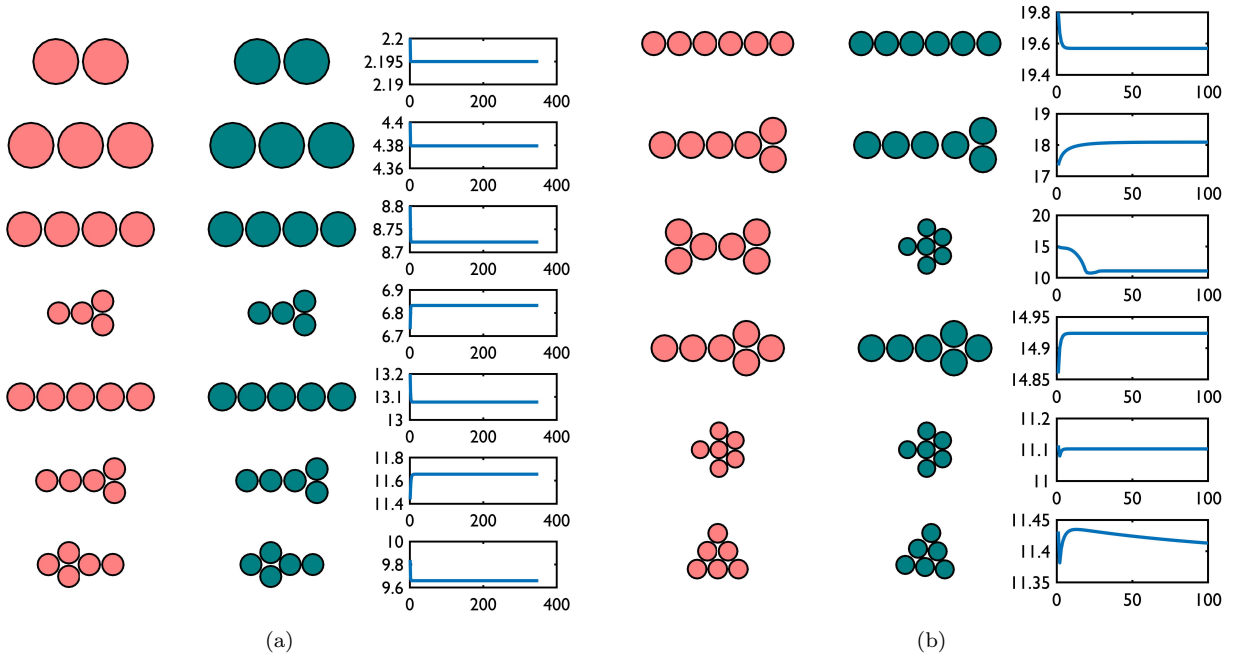


Figure 3: Structures assembled by Shen et al.<sup>3</sup>, which are not stable steady states of the governing equations: their shapes change upon perturbation (see figure 4 in Manuscript). Without any perturbation, these structures (or its mirror image) are steady state solutions to governing equations, except the third structure in 3b.

To systematically understand the possible steady states of the system and their stability

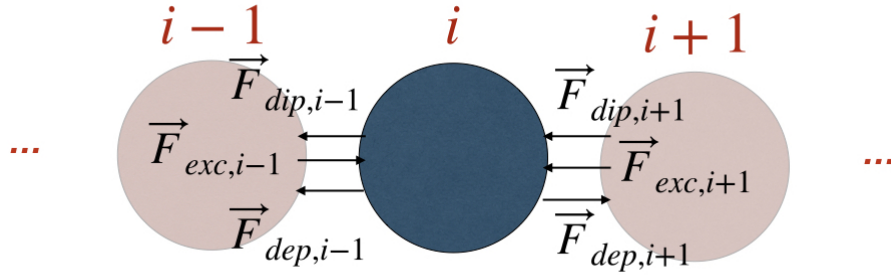


Figure 4: Forces in a generic linear assembly of droplets.

from the governing equations, one has to express them in terms of the distance between the droplet pairs. This is a very tedious task because, its complexity increases with the number of droplets in the assembly and the number of interactions governing the dynamics. Even if the equations that govern the change of shape of the droplet assembly are derived, one has to linearize the equations about the steady state and analyze the eigen spectrum. While this may shed light into the stability due to infinitesimally small perturbations. It is difficult to get a definite picture of the instability to small finite perturbation ( $\approx R/10$  used in our numerical study; often the case in reality).

## 2.2 Force balance in simple geometries

Though a systematic approach to the understanding/identifying the steady states is beyond the scope of the article, it is possible to get an intuitive picture of how the forces work in re-arranging the droplets to attain a certain shape for a few selected examples. In the sections to follow, we show how the forces are balanced in linear and triangular assemblies. This section is a qualitative study of the force-balance problem, intended to give the reader an intuitive feel for the forces at play.

### 2.2.1 Linear assemblies

In a perfectly linear assembly of droplets, aligned with the background flow (x-direction), forces are constrained to the x-axis. Figure 4, shows a linear assembly with forces on the  $i^{th}$  droplet due to its immediate neighbors. This allows the linear system of droplets to remain linear. Now even in this configuration, instability can arise if the forces tend to separate them indefinitely. However, the repulsive forces (Eq 5 of manuscript) are short ranged and depletion forces hold the droplets together. The dipole forces only result in slowing down of the entire assembly as a whole. However, once perturbed by moving one of the droplets away in the perpendicular direction, one can immediately see that the y-forces will set in to disturb the droplets taking them to a new steady state.

### 2.2.2 Triangular assemblies

An (equilateral) triangular configuration with the orientation as shown in figure 5a is unstable to the forces in the system and droplets re-arrange to yield its mirror image as shown in

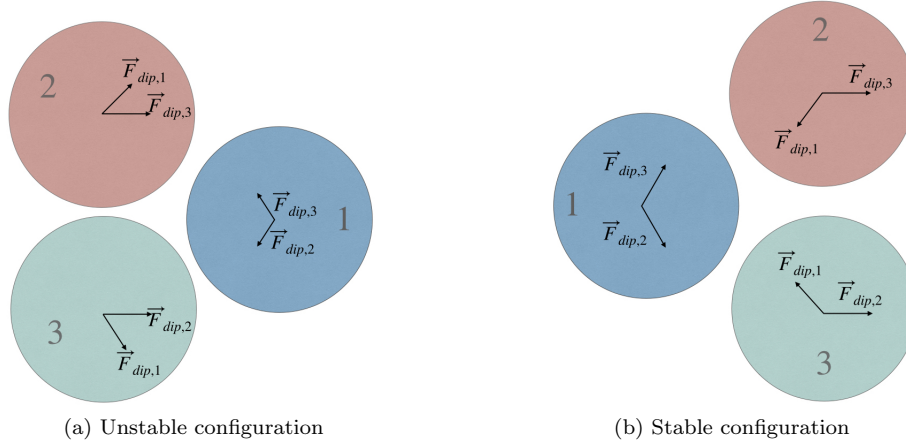


Figure 5: Forces in a triangular configuration of droplets.

figure 5b which is stable. In what follows, we will try to understand the stability problem qualitatively.

If the depletion forces were very strong, then the dipole forces will not be able to result in any re-arrangement and the configuration in figure 5a will also be stable. However, for the values of corresponding to the strengths of the forces used (refer to Shen et al<sup>3</sup>, for details on the parameter values used), the dipole forces due to the 1<sup>st</sup> and 3<sup>rd</sup> droplets are not balanced by the net attractive force due to the depletion interactions that keeps the droplet assembly compact. Which forces the 2<sup>nd</sup> droplet to slide over 1. Similarly 3<sup>rd</sup> droplet also has unbalanced forces that result in sliding to the right. This causes a transition to the configuration in figure 5b. In its new configuration, the forces are balanced by the depletion interactions and the configuration remains stable. In the absence of these attractive forces, the droplets (1 and 2) would have drifted indefinitely.

### 3 Details of the numerical simulations

Two classes of models are described in the manuscript (sections 2.1 and 2.2). The codes for both these models can be found at <https://github.com/DannyRajMasila/Hydrodynamics-droplet-ensembles>.

#### 3.1 Case 1: Long-range interaction dominant

The model described in Section 2.1 is similar to that in Shen et al<sup>3</sup>. They reported a range of possible shapes that were assembled and fused. We have numbered and characterized all of the shapes reported appropriately. With the codes provided in the online repository it is possible for one to study the steady state dynamics of these shapes.

The parameters used are identical as in ref<sup>3</sup>:  $R = 25 \times 10^{-6}$ ;  $Y = 0.5$ ;  $K = 1$ ;  $W = 1000 \times 10^{-6}$ ;  $H = 500 \times 10^{-6}$ .

#### 3.2 Case 2: Short-range interaction dominant

The model described in Section 2.2 and the parameters used for simulations are similar to that in ref<sup>4</sup>. The channel geometry is diverging and straight and are characterized by two

parameters,  $H = 0.0025$ , the height of the straight section and  $\alpha = 0.0016$ , the length across which the channel diverges from a height comparable to the size of the droplet to  $H$ .

The parameters used are identical as in ref<sup>4</sup>:  $\mu = 0.019$ ;  $R = 1.09 \times 10^{-4}$ ;  $k_f = 6\pi\mu R$ ;  $k_1 = 0.25$ ;  $\beta = 1$ ;  $k_d = 3 \times 6\pi\mu R^2$ ;  $k_b = 5 \times 6\pi\mu R^2$ ;

## References

- [1] R. H. Davis, J. a. Schonberg and J. M. Rallison, *Physics of Fluids A: Fluid Dynamics*, 1989, **1**, 77.
- [2] I. Wolfram Research, *Mathematica*, 2019.
- [3] B. Shen, J. Ricouvier, F. Malloggi and P. Tabeling, *Advanced Science*, 2016, **3**, 1600012.
- [4] M. Danny Raj and R. Rengaswamy, *Microfluidics and Nanofluidics*, 2014, **17**, 527–537.